

Spin asymmetries in $\gamma N \rightarrow \bar{K}^* \Theta^+$

Yongseok Oh,^{1,2,*} Hungchong Kim,^{2,†} and Su HOUNG Lee^{2,‡}

¹*Thomas Jefferson National Accelerator Facility,
12000 Jefferson Avenue, Newport News, VA 23606, U.S.A.*

²*Institute of Physics and Applied Physics,
Yonsei University, Seoul 120-749, Korea*

(Dated: November 20, 2018)

Abstract

The photoproduction processes of the exotic $\Theta^+(1540)$ baryon and the \bar{K}^* meson from the nucleon targets, i.e., $\gamma n \rightarrow K^{*-} \Theta^+$ and $\gamma p \rightarrow \bar{K}^{*0} \Theta^+$, are investigated in a hadronic model. We consider K and K^* exchanges as well as the s and u channel nucleon and Θ terms. Various spin asymmetries together with cross sections are first computed in order to study the production mechanisms and the parity of the $\Theta^+(1540)$ baryon. Within the uncertainties arising from the model-dependence of the production mechanisms and several coupling constants, we find that some target-recoil double spin asymmetries, $C_{xx'}^{\text{TR}}$ and $C_{xz'}^{\text{TR}}$, are sensitive to the parity of Θ^+ . In addition, the parity asymmetry of this reaction on the neutron target, which can be obtained by analyzing K^* decay distribution, is found to be useful to estimate the $K^* N \Theta$ coupling.

PACS numbers: 13.60.Rj, 13.60.-r, 14.20.Jn

Keywords: Θ^+ baryon, K^* photoproduction, spin asymmetries

arXiv:hep-ph/0312229v3 16 Sep 2004

*Electronic address: yoh@physast.uga.edu; Present address: Department of Physics and Astronomy, University of Georgia, Athens, GA 30602, U.S.A.

†Electronic address: hung@phya.yonsei.ac.kr

‡Electronic address: suhoun@phya.yonsei.ac.kr

I. INTRODUCTION

Since the discovery of the $\Theta^+(1540)$ by the LEPS Collaboration at SPring-8 [1], there have been a lot of experimental and theoretical studies for the exotic baryons. Experimentally, the observation of the $\Theta^+(1540)$ has been confirmed by many other experiments [2, 3, 4, 5, 6, 7, 8], of which results are summarized in Table I. The decay width of the $\Theta^+(1540)$ is found to be small but, due to the limitation in the detector resolution of those experiments, only its upper bound is known until now. Since the $\Theta^+(1540)$ has positive strangeness, its minimal quark content is $(uudd\bar{s})$ and so an exotic state. Furthermore, the NA49 Collaboration at CERN reported an evidence for the existence of another exotic Ξ baryon with a mass of 1.862 GeV, whose isospin is expected to be $3/2$ [9].

Theoretically, the chiral soliton model of Ref. [10] predicted a narrow pentaquark Θ^+ baryon at a mass of 1.53 GeV, which forms the baryon antidecuplet with the exotic Ξ particle. Such states are also anticipated in SU(3) Skyrme models, which allow all possible SU(3) representation of baryons [11, 12].¹ Although there is no quark degrees of freedom in soliton models, the positive strangeness of the Θ^+ implies the existence of a strange anti-quark in its wavefunction and hence the Θ^+ is interpreted as a pentaquark state in the quark model description. Exotic hadrons have been a challenge for hadron models and they are expected to widen our understanding of the hadron structure [13]. Viewing pentaquark baryons containing four quarks and one anti-quark, one finds that such baryons can form singlet, octet, decuplet, antidecuplet, 27-plet, and 35-plet, namely,

$$\mathbf{3} \otimes \mathbf{3} \otimes \mathbf{3} \otimes \mathbf{3} \otimes \bar{\mathbf{3}} = \mathbf{35} + (3)\mathbf{27} + (2)\bar{\mathbf{10}} + (4)\mathbf{10} + (8)\mathbf{8} + (3)\mathbf{1}, \quad (1)$$

as shown in Fig. 1, where the numbers in parentheses are the number of multiplicity. Then the Θ baryon that carries hypercharge $Y = +2$ can be a member of $\bar{\mathbf{10}}$, $\mathbf{27}$, or $\mathbf{35}$. However, depending on the multiplets, it has different isospin, namely, the antidecuplet contains isoscalar ($I = 0$) Θ , while the 27-plet and 35-plet contain the isovector ($I = 1$) Θ_1 and isotensor ($I = 2$) Θ_2 particles, respectively. Thus, the isospin measurement can answer the question in which multiplet the $\Theta^+(1540)$ resides. In this respect, the SAPHIR experiment [4] and the HERMES experiment [8], which report no evidence for a signal of the $\Theta^{++}(1540)$ in the K^+p invariant mass distribution in the γp and ed reactions, strongly support that the

Basic reaction	$M(\Theta^+)$ in MeV	$\Gamma(\Theta^+)$ in MeV	Collaboration/Reference
$\gamma n \rightarrow K^+K^-n$	1540 ± 10	≤ 25	LEPS [1]
$K^+Xe \rightarrow K^0pXe'$	1539 ± 2	≤ 9	DIANA [2]
$\gamma d \rightarrow K^+K^-pn$	1542 ± 5	≤ 21	CLAS [3]
$\gamma p \rightarrow K^+K_s^0n$	$1540 \pm 4 \pm 2$	≤ 25	SAPHIR [4]
$\gamma p \rightarrow \pi^+K^-K^+n$	1537 ± 10	≤ 31	CLAS [5]
$\nu_\mu(\bar{\nu}_\mu) + A \rightarrow \mu^-(\mu^+)pK_s^0X$	1533 ± 5	≤ 20	BBCN [6]
$\gamma p \rightarrow \pi^+K^-K^+n$	1555 ± 10	≤ 26	CLAS [7]
$ed \rightarrow pK_s^0X$	$1528 \pm 2.6 \pm 2.1$	$13 \pm 9 \pm 3$	HERMES [8]

TABLE I: Summary of the experimental data for the $\Theta^+(1540)$ baryon.

¹ Therefore, the SU(3) Skyrme model contains not only the pentaquarks but the heptaquarks and etc.

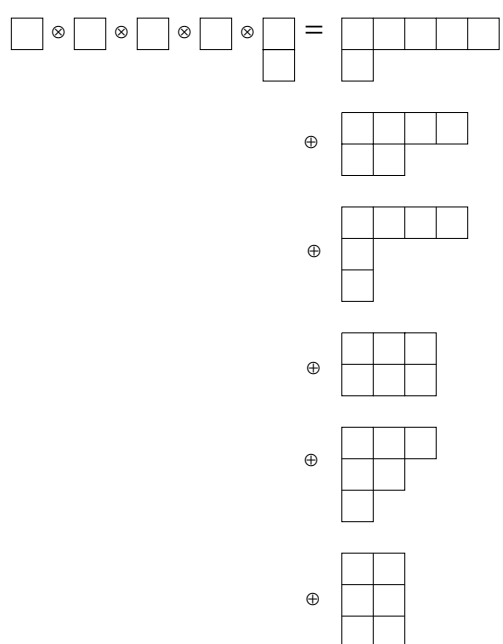
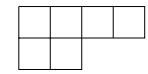
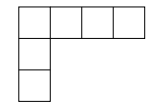
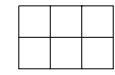
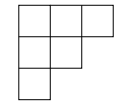
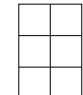
	Dim.	multi.	
	35	(1)	
\oplus 	27	(3)	
\oplus 	10	(4)	
\oplus 	$\bar{\mathbf{10}}$	(2)	
\oplus 	8	(8)	
\oplus 	1	(3)	

FIG. 1: Pentaquark baryons in the quark model. The numbers in parentheses are the multiplicity.

$\Theta^+(1540)$ is an isosinglet and hence it belongs to antidecuplet, which is also supported by the KN scattering data analyses of Ref. [14]. The low mass of the exotic Ξ states [9] also seems to support the antidecuplet nature of the $\Theta^+(1540)$ and $\Xi(1862)$. (See also Ref. [15] for a critical discussion about $\Xi(1862)$.)

However, the properties of the $\Theta^+(1540)$, especially its structure and quantum numbers, are yet to be clarified. As for the structure of the Θ^+ , there have been many suggestions in addition to the soliton models. In Ref. [16], Karliner and Lipkin suggested triquark-diquark model, where the (ud) diquark and the $(uds\bar{s})$ triquark form the Θ^+ . In Ref. [17], Jaffe and Wilczek advocated diquark-diquark-antiquark model so that the Θ^+ is a system of (ud) - (ud) - \bar{s} . In this model, they also considered the mixing of the pentaquark antidecuplet with the pentaquark octet, which makes it different from the $SU(3)$ soliton models where the octet describes the normal baryon octet. Assuming that the nucleon and Σ analogues are in the ideal mixing of the octet and antidecuplet, the nucleon analogue is then identified as the Roper resonance $N(1440)$.² In these correlated quark configurations, the color-flavor-spin wavefunction analyses favor the even-parity of the $\Theta^+(1540)$, which is consistent with the soliton model prediction. More discussions on the quark model predictions based on the diquark picture can be found, e.g., in Refs. [18, 21, 22]. Predictions on the antidecuplet spectrum in various quark models can be found, e.g., in Refs. [23, 24, 25, 26, 27, 28].

² In Ref. [18], it was pointed out that the Roper resonance $N(1710)$ cannot be a *pure antidecuplet state* due to $SU(3)$ symmetric interactions and U -spin conservation. The antidecuplet cannot couple to decuplet and meson octet while $N(1710)$ has a large branching ratio into the $\pi\Delta$ channel. Therefore, mixing with other multiplets is required to identify the $N(1710)$ as a pentaquark crypto-exotic state. However recent studies on the ideal mixing of antidecuplet with pentaquark octet show that the ideally mixed state still has vanishing coupling with the $\pi\Delta$ channel [19, 20].

Other theoretical investigations on the structure of Θ^+ and baryon antidecuplet include soliton models [29, 30, 31, 32, 33], QCD sum rules [34, 35, 36], large N_c QCD [37], and lattice calculation [38]. Another approach is to explain the Θ^+ as a KN or $K\pi N$ bound state [39]. Therefore, understanding the Θ^+ properties is essential to test those models. The production of Θ^+ can also be investigated in heavy-ion collisions as discussed in Ref. [40]. In this case, the Θ^+ yield is expected to carry informations on the early stage of the heavy ion collisions because of relatively weak interactions of Θ^+ with the hadrons produced in the collisions. But the results would be dependent on the detailed structure of Θ^+ .

Among the properties of $\Theta^+(1540)$, the parity quantum number is one of the important issues to be settled. If one assumes that all the quarks of the Θ^+ are in the S wave ground state, it is natural to expect the odd-parity for Θ^+ [25, 34, 36, 38]. However, if the quarks are strongly correlated, the P wave state is expected to have a lower energy so that the observed Θ^+ has even-parity [16, 17], which is consistent with the soliton model prediction [10]. This is also consistent with the quark potential model calculations [26], where the flavor-spin interaction plays an important role to give a lower mass to the P wave state. In this respect, it is interesting to recall the models for heavy pentaquarks, where an issue is whether the non-strange heavy pentaquarks like Θ_c^0 and Θ_b^+ are stable against strong decays [41]. In the bound state model of Skyrmion [42], such heavy pentaquarks are described as soliton-heavy-meson bound states. Although the Θ^+ cannot be a bound state of KN [31], a system like $\overline{D}N$ or BN can form bound states due to the heavy mass of D and B mesons. Then the pentaquark masses are lower than the thresholds so their decays by strong interactions are not allowed energetically. The detailed model calculation can be found in Ref. [43], where the heavy vector mesons are introduced to satisfy the heavy quark symmetry. The results show that the relative P wave state is the ground state so that the lowest Θ_c^0 and Θ_b^+ states have even-parity. Therefore one would expect even-parity Θ^+ unless level inversion occurs by the lighter mass of the kaon.

Nevertheless, the parity of the Θ^+ should be determined unambiguously by experiments through its production and decay processes.³ The production processes of the Θ^+ baryon have been investigated by several groups. In Refs. [44, 45], the total cross sections of Θ^+ production in photon-nucleon, meson-nucleon, and nucleon-nucleon reactions were discussed and obtained. It is then improved by including the tensor coupling terms for photon-nucleon interaction [46] and K^* exchanges [47]. The obtained results show that the cross sections for the odd-parity Θ^+ are much smaller than those for the even-parity. Based on the SU(3) symmetric Lagrangian of Ref. [18], the Θ^+ production processes in the KN and NN reactions were also discussed in Ref. [48] and the cross section of the $\gamma p \rightarrow \pi^+ K^- \Theta^+$ reaction was obtained in Ref. [49]. In order to determine the parity of the Θ^+ , various polarization observables in the $K^+ p \rightarrow \pi^+ K^+ n$ reaction [50], $\gamma n \rightarrow K^- \Theta^+$ [51], $\gamma n \rightarrow K^- K^+ n$ [52], and $p+p \rightarrow \Sigma + \Theta$ [53] reactions have been suggested and shown to be sensitive to the parity of the Θ^+ . As a continuation of our works on the Θ^+ production processes [47, 48], we investigate $\gamma N \rightarrow \overline{K}^* \Theta^+$ in this paper. In particular, we investigate the production mechanisms and various spin asymmetries of the $\gamma n \rightarrow K^{*-} \Theta^+$ and $\gamma p \rightarrow \overline{K}^{*0} \Theta^+$ reactions, which can be experimentally studied, e.g., at Thomas Jefferson National Accelerator Facility and SPring-8. By doing so, we also study the dependence of the spin observables on the parity of the Θ^+ . To be consistent with previous efforts for the Θ production in the literature, we consider in this

³ The spin-parity of the Θ^+ can be measured kinematically from the distribution of its decay into KN if the polarization of the outgoing nucleon is detected, which is, however, very difficult at present.

work only the elementary processes containing the well-known resonances in the intermediate state. Further development including higher resonances will be necessary in future though the calculation is limited by their unknown interactions with the Θ . Nevertheless, we discuss briefly how higher resonances can affect our results.

This paper is organized as follows. In Sec. II, we discuss the effective Lagrangians for the $\gamma + N \rightarrow \bar{K}^* + \Theta^+$ reactions with ($N = p, n$). The coupling constants and the production amplitudes are then computed depending on the parity of the Θ^+ . Section III shows the results for cross sections and various spin asymmetries, and their physical interpretations are discussed. The results are summarized in Sec. IV.

II. PRODUCTION MECHANISMS

Throughout this paper, we assume that the $\Theta^+(1540)$ has the quantum numbers, $J = 1/2$ and $I = 0$, and belongs to baryon antidecuplet.⁴ We give the results depending on the parity of the Θ^+ so that various spin asymmetries can be used to study not only the production mechanisms but also the parity of the $\Theta^+(1540)$. The reactions that are investigated in this paper are

$$\gamma + n \rightarrow K^{*-} + \Theta^+ \quad \text{and} \quad \gamma + p \rightarrow \bar{K}^{*0} + \Theta^+. \quad (2)$$

For the production mechanisms, we consider the tree diagrams as shown in Figs. 2 and 3. As in Refs. [47, 48], we consider the lowest baryons for the intermediate state of the s - and u -channel diagrams. Thus, we do not consider the nucleon resonances in the s -channel diagrams. Note that the Δ resonances in the intermediate state are not allowed by isospin. Similarly, isovector Θ_1 can contribute through the u -channel diagrams but its existence is still not established, so its contribution will not be considered in this study. Isotensor Θ^{**} cannot contribute by isospin conservation. In t -channel diagrams, we consider the K and K^* exchanges. But we do not consider the exchanges of higher K meson resonances like axial-vector $K_1(1270)$ meson. Although its radiative decay width into K meson is measured recently [55], there is no information to constrain its couplings to the nucleon and the Θ^+ as well as its decay into $K^*\gamma$. The role of such heavier meson exchanges can be studied when experimental data for various Θ^+ production processes are precise enough. It should be also noted that the t -channel diagram for $\gamma + p \rightarrow \bar{K}^{*0} + \Theta^+$ contains the K exchange only, while $\gamma + n \rightarrow K^{*-} + \Theta^+$ contains K and K^* exchanges in t channel.

The momenta of the incoming photon, the nucleon, the outgoing \bar{K}^* , and the Θ^+ are k , p , q , and p' , respectively. The Mandelstam variables are $s = (k + p)^2$, $t = (k - q)^2$ and $u = (p - q)^2$. In the c.m. frame, the momenta are given by $k = (\nu, \mathbf{k})$, $p = (E_N, -\mathbf{k})$, $q = (E_V, \mathbf{q})$ and $p' = (E_\Theta, -\mathbf{q})$ as shown in Fig. 4, which also defines the scattering angle θ and the helicities of the particles.

The effective Lagrangians containing $\Theta^+(1540)$ are obtained from the SU(3) symmetric Lagrangian for the interactions of the baryon antidecuplet with the meson octet and baryon octet [18],

$$\mathcal{L}_{\bar{D}PB} = g \bar{T}_{jkl} P_m^j B_n^k \epsilon^{lmn} + \text{H.c.}, \quad (3)$$

where T^{ijk} is the baryon antidecuplet, P_m^j the pseudoscalar/vector meson octet and B_n^k the

⁴ If it has isospin 2 [54], it would have very different production mechanisms.

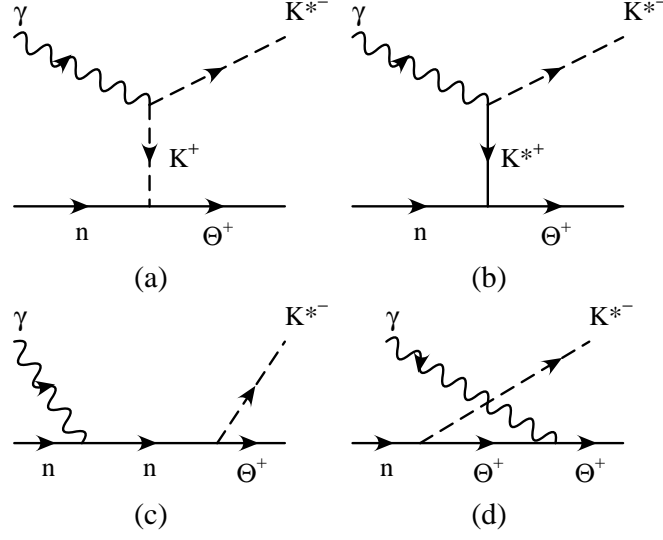


FIG. 2: Feynman diagrams for $\gamma n \rightarrow K^{*-}\Theta^+$.

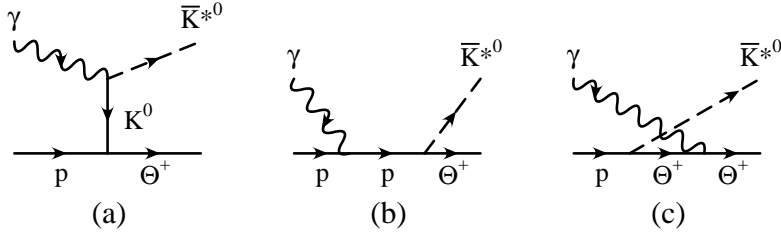


FIG. 3: Feynman diagrams for $\gamma p \rightarrow \bar{K}^{*0}\Theta^+$.

baryon octet. With the proper Lorentz structure of the interactions, this leads to

$$\mathcal{L}_{KN\Theta}^{\pm} = g_{KN\Theta} \bar{\Theta} \Gamma^{\pm} \bar{K}^c N + \text{H.c.}, \quad (4)$$

$$\mathcal{L}_{K^*N\Theta}^{\pm} = g_{K^*N\Theta} \bar{\Theta} \left(\Gamma_{\mu}^{\pm} \bar{K}^{*c\mu} - \frac{\kappa_{K^*N\Theta}^T}{M_N + M_{\Theta}} \Gamma^{\mp} \sigma^{\mu\nu} \partial_{\nu} \bar{K}_{\mu}^{*c} \right) N + \text{H.c.}, \quad (5)$$

where

$$\begin{pmatrix} \Gamma^+ \\ \Gamma^- \end{pmatrix} = \begin{pmatrix} i\gamma_5 \\ 1 \end{pmatrix}, \quad \begin{pmatrix} \Gamma_{\mu}^+ \\ \Gamma_{\mu}^- \end{pmatrix} = \begin{pmatrix} \gamma_{\mu} \\ i\gamma_5 \gamma_{\mu} \end{pmatrix}, \quad (6)$$

and

$$N = \begin{pmatrix} p \\ n \end{pmatrix}, \quad K^c = \begin{pmatrix} \bar{K}^0 \\ -K^- \end{pmatrix}, \quad K^{*c} = \begin{pmatrix} \bar{K}^{*0} \\ -K^{*-} \end{pmatrix}. \quad (7)$$

The upper (lower) sign of $\mathcal{L}_{KN\Theta}^{\pm}$ and $\mathcal{L}_{K^*N\Theta}^{\pm}$ is for the even (odd) parity Θ^+ . The Lagrangian of the $\gamma\Theta\Theta$ interaction is given by

$$\mathcal{L}_{\Theta\Theta\gamma} = -e\bar{\Theta} \left[A_{\mu} \gamma^{\mu} - \frac{\kappa_{\Theta}}{2M_{\Theta}} \sigma_{\mu\nu} \partial^{\nu} A^{\mu} \right] \Theta, \quad (8)$$

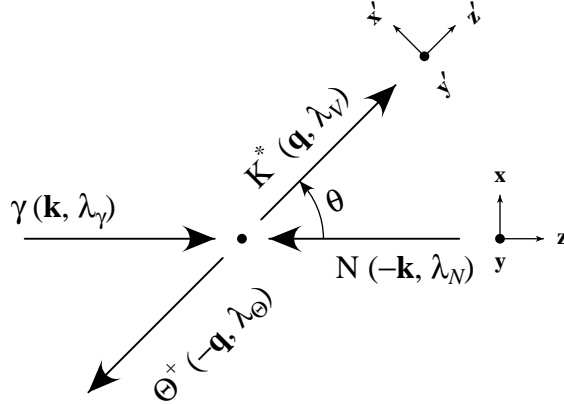


FIG. 4: The coordinate system and kinematic variables in the $\gamma + N \rightarrow \bar{K}^* + \Theta$ reaction.

where κ_Θ is the anomalous magnetic moment of Θ^+ . Other interactions needed to compute the diagrams of Figs. 2 and 3 are

$$\mathcal{L}_{NN\gamma} = -e\bar{N} \left[A_\mu \gamma^\mu \frac{1 + \tau_3}{2} - \frac{1}{4M_N} \{ \kappa_p + \kappa_n + \tau_3(\kappa_p - \kappa_n) \} \sigma_{\mu\nu} \partial^\nu A^\mu \right] N, \quad (9)$$

$$\mathcal{L}_{K^*K\gamma} = g_{K^*K\gamma} \varepsilon^{\mu\nu\alpha\beta} \partial_\mu A_\nu (\partial_\alpha K_\beta^{*-} K^+ + \partial_\alpha \bar{K}_\beta^{*0} K^0) + \text{H.c.}, \quad (10)$$

$$\mathcal{L}_{K^*K^*\gamma} = -ieA^\mu \{ K^{*- \nu} (\partial_\mu K_\nu^{*+} - \partial_\nu K_\mu^{*+}) - (\partial_\mu K_\nu^{*-} - \partial_\nu K_\mu^{*-}) K^{*+ \nu} \}. \quad (11)$$

The coupling constants are determined as follows. First, the coupling constant $g_{KN\Theta}$ can be determined by the decay width of the $\Theta^+(1540)$. However, only its upper bound is known at present, so we have to rely on model predictions or analyses of other reactions. In the chiral soliton model, the decay width $\Gamma(\Theta)$ was estimated to be 15 MeV [10] or 5 MeV [56]. Recent analyses on KN scattering data favor such a small decay width of the Θ^+ [57], but a much smaller decay width, namely, 1 MeV or even less, is claimed by Refs. [14]. In this study, leaving its determination to future experimental investigations, we use $\Gamma(\Theta) = 1$ MeV, which gives

$$g_{KN\Theta} = 0.984, \quad (12a)$$

for the even-parity Θ^+ , and

$$g_{KN\Theta} = 0.137, \quad (12b)$$

for the odd-parity Θ^+ . There is no direct information for $g_{K^*N\Theta}$, but using quark model wavefunctions for Θ^+ one can estimate the ratio $g_{K^*N\Theta}/g_{KN\Theta}$, which gives

$$g_{K^*N\Theta}/g_{KN\Theta} = \sqrt{3}, \quad (13a)$$

for the even-parity Θ^+ [19, 58], and

$$g_{K^*N\Theta}/g_{KN\Theta} = 1/\sqrt{3}, \quad (13b)$$

for the odd-parity Θ^+ [25]. In this paper, we use the above values for our numerical calculation. It also shows that the ratio, $g_{K^*N\Theta}/g_{KN\Theta}$, is quite dependent of the parity of Θ^+ and hence can be a tool to probe the Θ^+ parity. Some qualitative estimate on this ratio can be obtained by measuring the spin asymmetries in the $\gamma N \rightarrow \bar{K}^* \Theta^+$ reaction as will be discussed below. As in Ref. [47], we take the tensor coupling, $\kappa_{K^*N\Theta}^T = 0$ keeping

in mind that the nonvanishing tensor coupling would affect especially the predictions for spin asymmetries. The anomalous magnetic moment κ_Θ of the Θ^+ , which should reveal the structure of the Θ^+ , depends on the hadron models [59]. But the results of Ref. [47] show that the sensitivity to the κ_Θ term is overwhelmed by the variation of the $g_{K^*N\Theta}$ coupling as long as $|\kappa_\Theta| < 1$. In this study we use $\kappa_\Theta = -0.9$ assuming that $\mu_\Theta \sim 0.1$ [59]. The anomalous magnetic moments of the nucleon are $\kappa_p = 1.79$ and $\kappa_n = -1.91$. For the $K^*K\gamma$ coupling, we use the experimental data for the K^* radiative decays as in Ref. [47], which gives $g_{K^*K\gamma}^0 = -0.388 \text{ GeV}^{-1}$ for the neutral decay and $g_{K^*K\gamma}^c = 0.254 \text{ GeV}^{-1}$ for the charged decay. Here the phases of $g_{K^*K\gamma}$ are fixed according to the SU(3) symmetry and vector meson dominance [61].

Now we consider the production amplitudes of $\gamma + N \rightarrow \bar{K}^* + \Theta^+$. The production amplitudes of this reaction are generally written in the form of

$$\mathcal{M} = \varepsilon_\nu^*(K^*) \bar{u}_\Theta(p') \mathcal{M}^{\mu\nu} u_p(p) \varepsilon_\mu(\gamma), \quad (14)$$

where ε 's are the polarization vectors of the K^* and photon. With the effective Lagrangians given above, the production amplitudes for $\gamma + n \rightarrow K^{*-} + \Theta^+$ shown in Fig. 2 read

$$\mathcal{M}_{(a)}^{\mu\nu} = \frac{g_{K^*K\gamma}^c g_{KN\Theta}}{t - M_K^2} \varepsilon^{\mu\nu\alpha\beta} k_\alpha q_\beta \Gamma^\pm F_{2(a)}(s, t, u), \quad (15a)$$

$$\begin{aligned} \mathcal{M}_{(b)}^{\mu\nu} &= \frac{eg_{K^*N\Theta}}{t - M_{K^*}^2} (q^\alpha g^{\mu\nu} - k^\nu g^{\mu\alpha} - 2q^\mu g^{\nu\alpha}) \left\{ g_{\alpha\beta} - \frac{1}{M_{K^*}^2} (k - q)_\alpha (k - q)_\beta \right\} \\ &\times \left\{ \Gamma^{\pm\beta} + \frac{i\kappa_{K^*N\Theta}^T}{M_N + M_\Theta} \Gamma^\mp \sigma^{\beta\delta} (k - q)_\delta \right\} F_{2(b)}(s, t, u), \end{aligned} \quad (15b)$$

$$\begin{aligned} \mathcal{M}_{(c)}^{\mu\nu} &= \frac{ieg_{K^*N\Theta}}{s - M_N^2} \frac{\kappa_n}{2M_N} \left(\Gamma^{\pm\nu} - \frac{i\kappa_{K^*N\Theta}^T}{M_N + M_\Theta} \Gamma^\mp \sigma^{\nu\alpha} q_\alpha \right) (\not{k} + \not{p} + M_N) \sigma^{\mu\beta} k_\beta \\ &\times F_{2(c)}(s, t, u), \end{aligned} \quad (15c)$$

$$\begin{aligned} \mathcal{M}_{(d)}^{\mu\nu} &= \frac{eg_{K^*N\Theta}}{u - M_\Theta^2} \left[\gamma^\mu + \frac{i\kappa_\Theta}{2M_\Theta} \sigma^{\mu\alpha} k_\alpha \right] (\not{p} - \not{q} + M_\Theta) \\ &\times \left(\Gamma^{\pm\nu} - \frac{i\kappa_{K^*N\Theta}^T}{M_N + M_\Theta} \Gamma^\mp \sigma^{\nu\beta} q_\beta \right) F_{2(d)}(s, t, u), \end{aligned} \quad (15d)$$

where $g_{K^*K\gamma}^c = 0.254 \text{ GeV}^{-1}$ is obtained from $\Gamma(K^{*\pm} \rightarrow K^\pm \gamma)$.

For $\gamma + p \rightarrow \bar{K}^{*0} \Theta^+$ reaction depicted in Fig. 3, we have

$$\mathcal{M}_{(a)}^{\mu\nu} = -\frac{g_{K^*K\gamma}^0 g_{KN\Theta}}{t - M_K^2} \varepsilon^{\mu\nu\alpha\beta} k_\alpha q_\beta \Gamma^\pm F_{3(a)}(s, t, u), \quad (16a)$$

$$\begin{aligned} \mathcal{M}_{(b)}^{\mu\nu} &= -\frac{eg_{K^*N\Theta}}{s - M_N^2} \left[\Gamma^{\pm\nu} - \frac{i\kappa_{K^*N\Theta}^T}{M_N + M_\Theta} \Gamma^\mp \sigma^{\nu\alpha} q_\alpha \right] (\not{k} + \not{p} + M_N) \\ &\times \left[\gamma^\mu + \frac{i\kappa_p}{2M_N} \sigma^{\mu\beta} k_\beta \right] F_{3(b)}(s, t, u), \end{aligned} \quad (16b)$$

$$\begin{aligned} \mathcal{M}_{(c)}^{\mu\nu} &= -\frac{eg_{K^*N\Theta}}{u - M_\Theta^2} \left[\gamma^\mu + \frac{i\kappa_\Theta}{2M_\Theta} \sigma^{\mu\alpha} k_\alpha \right] (\not{p} - \not{q} + M_\Theta) \\ &\times \left[\Gamma^{\pm\nu} - \frac{i\kappa_{K^*N\Theta}^T}{M_N + M_\Theta} \Gamma^\mp \sigma^{\nu\beta} q_\beta \right] F_{3(c)}(s, t, u), \end{aligned} \quad (16c)$$

where $g_{K^*K\gamma}^0 = -0.388 \text{ GeV}^{-1}$ is obtained from $\Gamma(K^{*0} \rightarrow K^0\gamma)$.

As in our previous calculations [47, 48], we employ the form factor of the form

$$F(r, M_{\text{ex}}) = \frac{\Lambda^4}{\Lambda^4 + (r - M_{\text{ex}}^2)^2}, \quad (17)$$

where M_{ex} is the mass of the exchanged particle and r is its momentum squared.

The amplitudes in Eqs. (15) and (16) satisfy the gauge invariance condition without form factors. However introducing different form factors at each vertex breaks gauge invariance. There are several recipes in restoring gauge invariance with the use of phenomenological form factors [47, 49], and the results depend on the employed form factors and the way to restore gauge invariance. In order to keep gauge invariance in a simple way, we use

$$F_{2(b)} = F_{2(d)} = \{F(t, M_{K^*})^2 + F(u, M_{\Theta})^2\} / 2, \quad F_{2(a)} = F(t, M_K)^2, \quad F_{2(c)} = F(s, M_N)^2, \quad (18)$$

and

$$F_{3(a)} = F(t, M_K)^2, \quad F_{3(b)} = F_{2(c)} = \{F(s, M_N)^2 + F(u, M_{\Theta})^2\} / 2. \quad (19)$$

This is an unsatisfactory aspect of this hadronic model approach, but it should be sufficient for this qualitative study. For the cutoff parameter, we use $\Lambda = 1.8 \text{ GeV}$ as in Refs. [47, 48].

III. RESULTS

Before presenting the results for the $\gamma N \rightarrow \bar{K}^* \Theta^+$ reaction, let us discuss the uncertainties arising from neglecting intermediate baryon resonances in s and u channels. The production mechanisms include the s and u channel diagrams as shown in Figs. 2(c,d) and 3(b,c). In addition to the ground state resonances that we currently have, the nucleon resonances (N^*) can intermediate the s channel diagrams and Θ excitations can contribute to the u channel. Those contributions, in principle, should be included as some of the physical quantities, especially some spin asymmetries, may be sensitive to such resonances as in the case of vector meson photoproduction [60]. At this stage, the possible contribution from Θ excitations can be ignored as their existence is not yet confirmed. As for the N^* contribution, if N^* belongs to the baryon antidecuplet, it contributes only to the neutron target case since it is not allowed for the proton target case due to U spin symmetry [13, 18]. This selection rule does not apply to the N^* belonging to other multiplets and it can contribute to both targets. Calculating such contributions, however, should be very limited by various unknown couplings. For example, the N^* contribution in the s channel contains rather unknown couplings of γNN^* and $\bar{K}^* \Theta N^*$. Additional uncertainties come from the unfixed width and mass of N^* . Instead of estimating the N^* contribution with such uncertainties, we include only the lowest and established states as the intermediate state of s and u channel diagrams. Thus, our results should be understood as a first estimate on the spin asymmetries in the $\gamma N \rightarrow \bar{K}^* \Theta$ reaction and such uncertainties should be kept in mind.⁵ Since the contributions from the s and u channel diagrams with excited states mostly contribute to large scattering angles, we restrict our investigation to small scattering angle region.

⁵ Such uncertainties are also present in other reaction studies such as $\gamma N \rightarrow \bar{K} N$ and $\gamma N \rightarrow K^+ K^- N$, while the $NN \rightarrow Y\Theta$ reaction study suffers from the uncertainties arising from the initial state interactions.

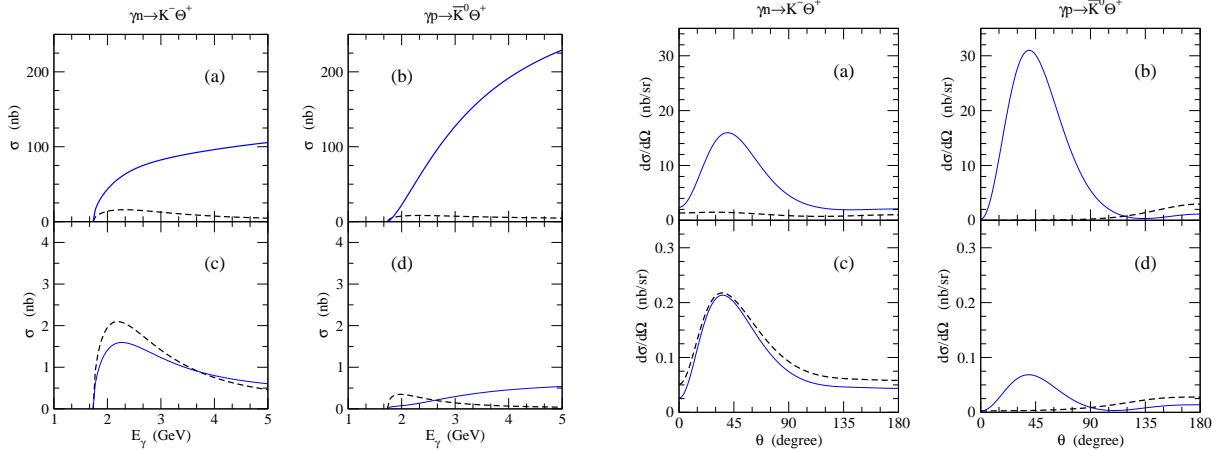


FIG. 5: Cross sections for $\gamma + N \rightarrow \bar{K} + \Theta^+$. Total cross sections (left panel) and differential cross sections at $E_\gamma = 3.0$ GeV (right panel). (a,c) for $\gamma + n \rightarrow K^- + \Theta^+$ and (b,d) for $\gamma + p \rightarrow \bar{K}^0 + \Theta^+$. In (a,b), even-parity is assumed for Θ^+ , and in (c,d), odd-parity of Θ^+ is assumed. The dashed lines are obtained with $g_{K^*N\Theta} = 0$, and the solid lines are with $g_{K^*N\Theta}/g_{KN\Theta} = \sqrt{3}$ ($1/\sqrt{3}$) for positive (negative) parity Θ^+ as in Eq. (13).

We now present the results for various physical quantities in the $\gamma + N \rightarrow \bar{K}^* + \Theta^+$ reaction based on the formalism given in the previous section. For this calculation, we use the couplings $g_{KN\Theta}$ and $g_{K^*N\Theta}$ as in Eqs. (12) and (13). Since the coupling constants are different from those of Ref. [47], we start with presenting the total cross sections and differential cross sections at $E_\gamma = 3$ GeV for $\gamma + N \rightarrow \bar{K} + \Theta^+$ in Fig. 5 obtained with the parameters given above. Shown in the left panel are the total cross sections and the right panel presents the results for the differential cross sections. The dashed lines are obtained with $g_{K^*N\Theta}/g_{KN\Theta} = 0$ and the solid lines are with the values of Eq. (13). The difference with the results of Ref. [47] arises from the different coupling constant $g_{KN\Theta}$ and the different phase in $g_{K^*K\gamma}^0$. This shows that the large value of the ratio $g_{K^*N\Theta}/g_{KN\Theta}$ in the case of even-parity Θ^+ leads to the dominance of K^* exchange in Θ^+ production process, which is characterized by a peak in the forward scattering angles near $\theta = \pi/4$. The contribution from u and s channels does not have a distinct peak structure. The N^* contribution, if it is included, is expected to have a nearly flat structure as it contributes through the s -channel only. Thus, the distinct peak structure observed near $\theta = \pi/4$ is a characteristic of the t -channel exchanges in this model and it would be interesting to see whether such structure survives within more sophisticated models with higher resonances in coupled channels.

A. Cross Sections

In Fig. 6, we present the total cross sections for $\gamma + N \rightarrow \bar{K}^* + \Theta$. Shown in Fig. 7 are the differential cross sections at $E_\gamma = 2.8$ GeV. The results show that the cross sections for the odd-parity Θ^+ production are much smaller than those for the even-parity Θ^+ production. This is because of the smaller coupling constants for the odd-parity Θ^+ . Figures 6 and 7 also show that the γp reaction has larger cross sections than the γn reaction when $g_{K^*N\Theta} = 0$. This can be easily understood from the fact that $|g_{K^*K\gamma}^0| > |g_{K^*K\gamma}^c|$ [61]. Specifically, without $K^*N\Theta$ interaction, we have the diagrams of Fig. 2(a) and 3(a) only. Therefore, the

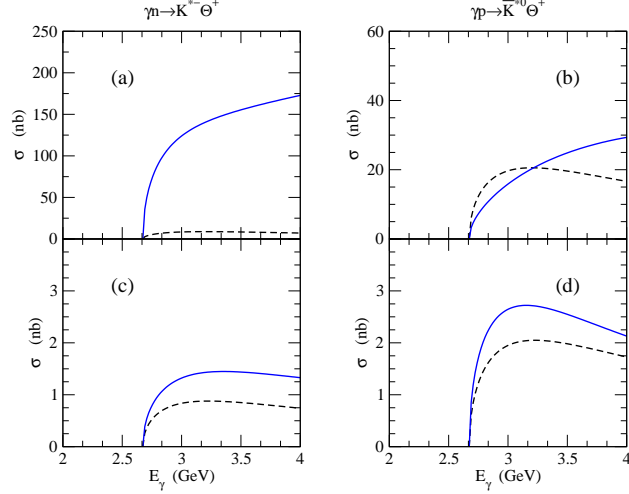


FIG. 6: Total cross sections for $\gamma + N \rightarrow \overline{K}^* + \Theta^+$. Notations are the same as in Fig. 5.

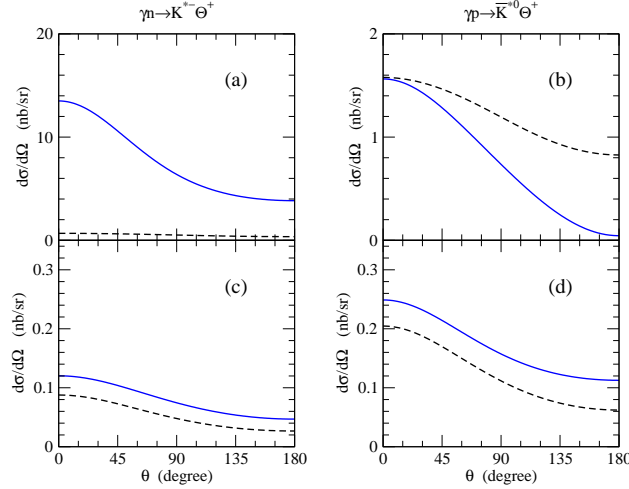


FIG. 7: Differential cross sections for $\gamma + N \rightarrow \overline{K}^* + \Theta^+$ at $E_\gamma = 2.8$ GeV. Notations are the same as in Fig. 5.

only difference between the two diagrams lies on the $K^*K\gamma$ couplings. Since the γp reaction has neutral kaon exchange, its cross section is larger than that for the γn reaction. However, when the $K^*N\Theta$ interaction is turned on, there is interference among the production amplitudes so that the cross sections depend on the magnitude of the $K^*N\Theta$ interaction. Another interesting observation is that the cross sections for $\gamma + N \rightarrow \overline{K}^* + \Theta^+$ are comparable to or even larger in some cases than those for the $\gamma + N \rightarrow \overline{K} + \Theta^+$ reaction. But we notice that the shape of the differential cross sections is different for $\gamma + N \rightarrow \overline{K}^* + \Theta^+$ and $\gamma + N \rightarrow \overline{K} + \Theta^+$. With nonzero $g_{K^*N\Theta}$ coupling, the K^* production is dominantly in forward angles while for the K , the production is peaked near the 45 degrees. This is mostly due to the fact that the role of the K and K^* exchanges is different in these reactions, e.g., in the γp reaction, the t -channel diagram has only K exchange in $\overline{K}^*\Theta^+$ production while in $\overline{K}\Theta^+$ production the diagram contains only K^* exchange. The forward peak in $\gamma + N \rightarrow \overline{K}^* + \Theta^+$ is expected to persist even when the N^* contribution is included. As

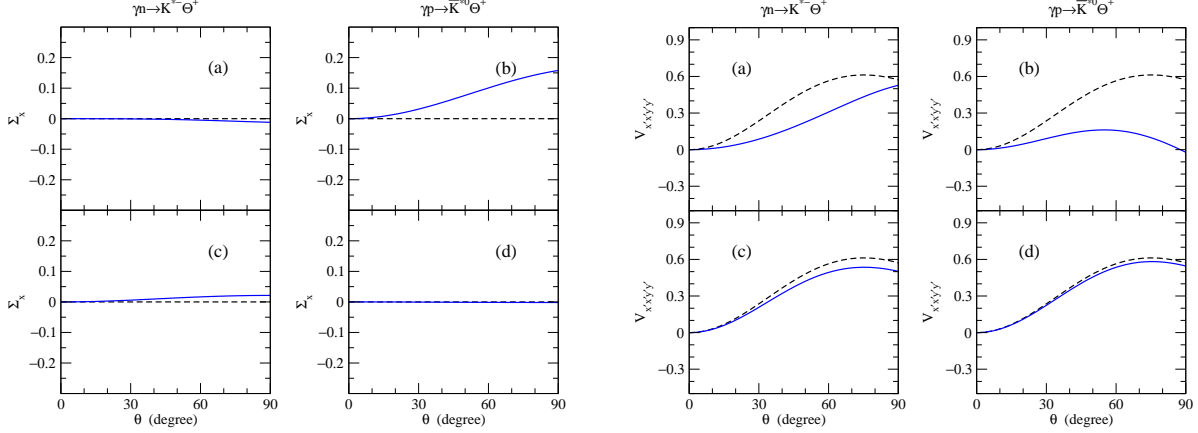


FIG. 8: Polarized photon beam asymmetry Σ_x (left panel) and vector meson (K^*) tensor asymmetry $V_{x'x'y'y'}$ (right panel) for $\gamma + N \rightarrow \bar{K}^* + \Theta^+$ at $E_\gamma = 2.8$ GeV. Notations are the same as in Fig. 5.

we have mentioned, the resonance contribution in u and s -channels is expected to change the shape in the backward angles. In fact, this contribution makes the solid curves in Fig.7 flattened in the backward angles. Thus, the N^* contribution, which contributes through the s -channel, is expected to change the shape mostly in the backward angles.

B. Single and Double Spin Asymmetries

We now compute several single and double spin asymmetries at $E_\gamma = 2.8$ GeV, of which definitions and explicit expressions can be found, e.g., in Ref. [62]. We first calculate single spin asymmetries: polarized photon beam asymmetry (analyzing power) Σ_x and tensor polarization asymmetry $V_{x'x'y'y'}$ of the produced K^* . As we have discussed, the contribution from the higher nucleon resonances would be important in spin asymmetries at large scattering angles. Therefore, we give our results only for *forward* scattering angle, $\theta < 90^\circ$. The polarized photon beam asymmetry is defined as

$$\Sigma_x = \frac{\sigma^\parallel - \sigma^\perp}{\sigma^\parallel + \sigma^\perp}, \quad (20)$$

where σ^\parallel (σ^\perp) is the differential cross section produced by a photon linearly polarized along the \hat{x} and (\hat{y}) axis. The definition of the tensor polarization asymmetry of the vector meson can be found, e.g., in Refs. [62, 63]. In Fig. 8, the results for Σ_x and $V_{x'x'y'y'}$ are presented. Here again, the dashed and solid lines are obtained with $g_{K^*N\Theta}/g_{KN\Theta} = 0$ and $\sqrt{3}$ ($1/\sqrt{3}$) for even (odd) parity of Θ^+ , respectively. Our results show the dependence of the single spin asymmetries on the production mechanisms.

Shown in Figs. 9–11 are the results for several double spin asymmetries. Here, we present the results for beam-target (Fig. 9) and target-recoil (Figs. 10 and 11) asymmetries. For their definitions, let us consider, e.g., beam-target double asymmetry C_{zz}^{BT} . The physical meaning of this asymmetry is

$$C_{zz}^{\text{BT}} = \frac{\sigma^{z,z} - \sigma^{z,-z}}{\sigma^{z,z} + \sigma^{z,-z}}, \quad (21)$$

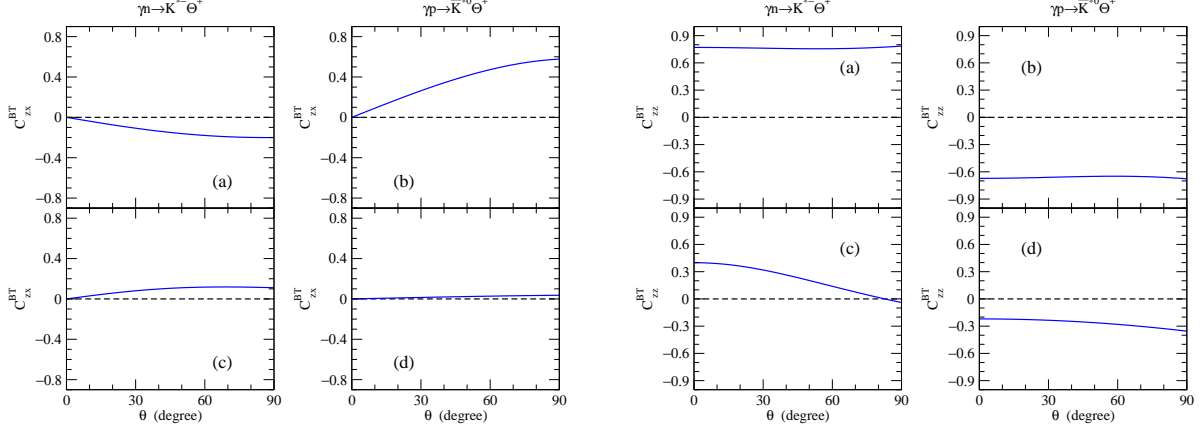


FIG. 9: Beam-target double asymmetries C_{zx}^{BT} (left panel) and C_{zz}^{BT} (right panel) for $\gamma + N \rightarrow \bar{K}^* + \Theta^+$ at $E_\gamma = 2.8$ GeV. Notations are the same as in Fig. 5.

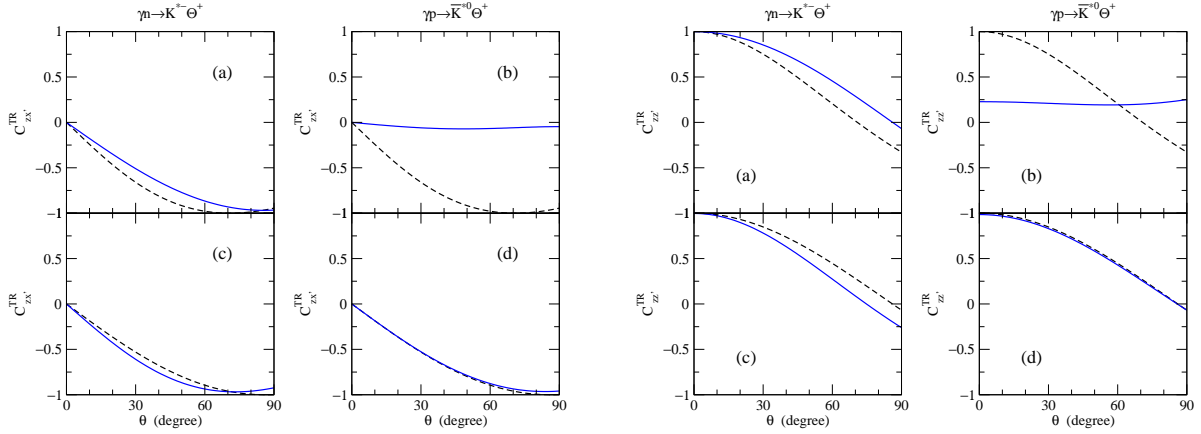


FIG. 10: Target-recoil double asymmetries C_{zx}^{TR} (left panel) and $C_{zz'}^{TR}$ (right panel) for $\gamma + N \rightarrow \bar{K}^* + \Theta^+$ at $E_\gamma = 2.8$ GeV. Notations are the same as in Fig. 5.

where the first z means the polarization of the photon beam, i.e., it is circularly polarized with helicity $+1$, and the second $\pm z$ denotes the direction of the target nucleon polarization. The reference frame is defined in Fig. 4. The other double polarizations are defined in a similar way [62]. The obtained results show that the asymmetries depend not only on the production dynamics but also on the Θ^+ parity.

The most interesting results are the target-recoil double asymmetries C_{zx}^{TR} and $C_{zz'}^{TR}$ shown in Fig. 11. These asymmetries for the proton targets, in particular, are very sensitive to the parity of the Θ^+ , as their dependence on the $K^*N\Theta$ interaction is relatively weak because of the absence of K^* exchange in t -channel. In order to understand the behavior of those asymmetries, let us consider the helicity amplitudes in the t -channel K exchange. The amplitudes contain

$$\begin{aligned} \bar{u}_\Theta(p', m_f) \gamma_5 u_N(p, m_i) &\propto A_1(s, t, u) \chi_\Theta^\dagger \boldsymbol{\sigma} \cdot \hat{\mathbf{p}} \chi_N - A_2(s, t, u) \chi_\Theta^\dagger \boldsymbol{\sigma} \cdot \hat{\mathbf{p}}' \chi_N, \\ \bar{u}_\Theta(p', m_f) u_N(p, m_i) &\propto B_1(s, t, u) \chi_\Theta^\dagger \chi_N - B_2(s, t, u) \chi_\Theta^\dagger \boldsymbol{\sigma} \cdot \hat{\mathbf{p}} \boldsymbol{\sigma} \cdot \hat{\mathbf{p}}' \chi_N, \end{aligned} \quad (22)$$

where χ 's are the Pauli spinors and A_i and B_i are some functions of the Mandelstam vari-

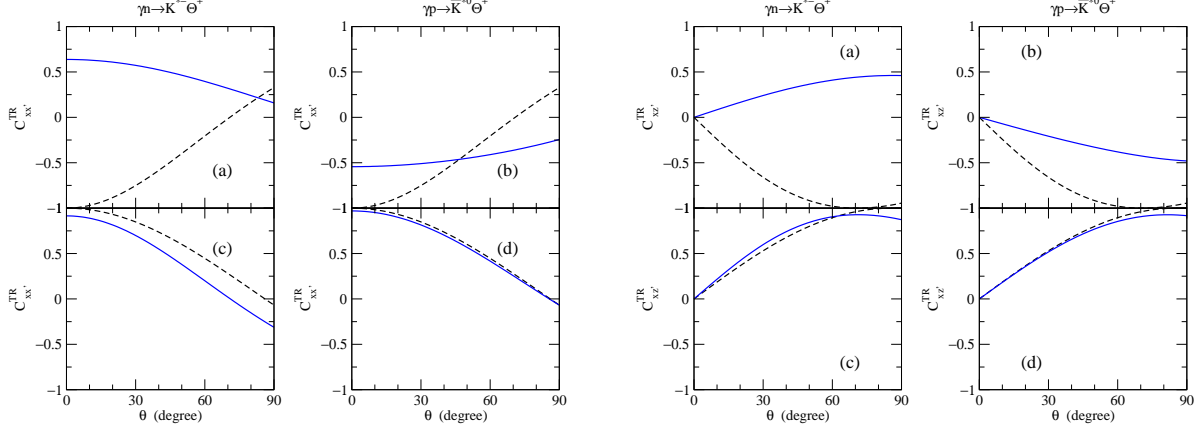


FIG. 11: Target-recoil double asymmetries $C_{xx'}^{\text{TR}}$ (left panel) and $C_{xz'}^{\text{TR}}$ (right panel) for $\gamma + N \rightarrow \bar{K}^* + \Theta^+$ at $E_\gamma = 2.8$ GeV. Notations are the same as in Fig. 5.

ables. Then in the c.m. frame (Fig. 4), $\hat{\mathbf{p}} = -\hat{\mathbf{z}}$, and at $\theta = \pi$ so that $\hat{\mathbf{p}}' = \hat{\mathbf{z}}$, we have

$$\begin{aligned}
\bar{u}_\Theta(p', m_f) \gamma_5 u_N(p, m_i) &\propto -[A_1(s, t, u) + A_2(s, t, u)] \chi_\Theta^\dagger \sigma_3 \chi_N \\
&= -[A_1(s, t, u) + A_2(s, t, u)] m_i \delta_{m_i, m_f}, \\
\bar{u}_\Theta(p', m_f) u_N(p, m_i) &\propto [B_1(s, t, u) + B_2(s, t, u)] \chi_\Theta^\dagger \chi_N \\
&= [B_1(s, t, u) + B_2(s, t, u)] \delta_{m_i, m_f}.
\end{aligned} \tag{23}$$

Furthermore, since

$$\begin{aligned}
C_{xx'}^{\text{TR}} &\propto \langle -\frac{1}{2} | \mathcal{M} | +\frac{1}{2} \rangle^* \langle +\frac{1}{2} | \mathcal{M} | -\frac{1}{2} \rangle + \langle -\frac{1}{2} | \mathcal{M} | -\frac{1}{2} \rangle^* \langle +\frac{1}{2} | \mathcal{M} | +\frac{1}{2} \rangle, \\
C_{xz'}^{\text{TR}} &\propto \langle +\frac{1}{2} | \mathcal{M} | +\frac{1}{2} \rangle^* \langle +\frac{1}{2} | \mathcal{M} | -\frac{1}{2} \rangle - \langle -\frac{1}{2} | \mathcal{M} | +\frac{1}{2} \rangle^* \langle -\frac{1}{2} | \mathcal{M} | -\frac{1}{2} \rangle,
\end{aligned} \tag{24}$$

in the form of $\langle \lambda_f | \mathcal{M} | \lambda_i \rangle$, where the sum over the other helicities is understood, and using Eq. (23) at $\theta \rightarrow \pi$, we can find that $C_{xx'}^{\text{TR}}$ has different sign depending on the parity of the Θ^+ and $C_{xz'}^{\text{TR}} = 0$ at $\theta = \pi$. This conclusion holds also at $\theta = 0$. Thus the results shown in Fig. 11 can be understood in this kinematic region. Of course, these results should be modified to some extent by including $K^*N\Theta$ interactions, but the results of Fig. 11 show that it does not change so much for the case of the proton targets at least in the forward scattering region. However, for the neutron targets, the interference between the two interactions is large so that the results are dependent on the $g_{K^*N\Theta}$ coupling constant. Although the target-recoil double asymmetries are very sensitive to the parity of the Θ^+ , experimental measurements of those asymmetries would be very hard because of the difficulties with identifying the helicity of Θ^+ .

C. Parity Asymmetry and Photon Asymmetry

We now consider the parity asymmetry P_σ and the photon asymmetry Σ_V in $\gamma + N \rightarrow \bar{K}^* + \Theta^+$. These asymmetries can be measured by observing the decay angular distribution of the \bar{K}^* vector meson produced by linearly polarized photon beams [64]. If we define $\tilde{\sigma}_\parallel$ and $\tilde{\sigma}_\perp$ as the cross sections for symmetric decay particle pairs, i.e., kaon and pion pairs,

produced parallel and normal to the photon polarization plane respectively, the photon polarization asymmetry Σ_V is defined by

$$\Sigma_V \equiv \frac{\tilde{\sigma}_{\parallel} - \tilde{\sigma}_{\perp}}{\tilde{\sigma}_{\parallel} + \tilde{\sigma}_{\perp}}, \quad (25)$$

which can be related to the density matrix elements of the K^* vector meson (when produced by linearly polarized photon beam) as

$$\Sigma_V = \frac{\rho_{11}^1 + \rho_{1-1}^1}{\rho_{11}^0 + \rho_{1-1}^0}. \quad (26)$$

The definitions for the density matrix $\rho_{\lambda\lambda'}^i$ can be found in Ref. [64].

Another interesting quantity is the parity asymmetry P_{σ} . This can be defined by decomposing the helicity amplitudes as

$$\mathcal{M} = \mathcal{M}^N + \mathcal{M}^U, \quad (27)$$

or

$$\mathcal{M}_{\lambda_V \lambda_{\Theta}, \lambda_{\gamma} \lambda_N}^{N/U} = \frac{1}{2} \{ \mathcal{M}_{\lambda_V \lambda_{\Theta}, \lambda_{\gamma} \lambda_N} \mp (-1)^{\lambda_V} \mathcal{M}_{-\lambda_V \lambda_{\Theta}, -\lambda_{\gamma} \lambda_N} \}. \quad (28)$$

This decomposition is from the observation that if only natural parity [$\eta = (-1)^j$, where η and j are the parity and spin of the exchanged particle] or only unnatural parity [$\eta = -(-1)^j$] exchange in the t -channel contributes, one has an additional symmetry to leading order in the incoming photon energy [65],

$$\begin{aligned} \mathcal{M}_{-\lambda_V \lambda_{\Theta}, -\lambda_{\gamma} \lambda_N} &= \pm (-1)^{\lambda_V - \lambda_{\gamma}} \mathcal{M}_{\lambda_V \lambda_{\Theta}, \lambda_{\gamma} \lambda_N} \\ &= \mp (-1)^{\lambda_V} \mathcal{M}_{\lambda_V \lambda_{\Theta}, \lambda_{\gamma} \lambda_N}, \end{aligned} \quad (29)$$

where the upper (lower) sign applies to natural (unnatural) parity exchange. Then one can decompose the cross sections due to natural and unnatural parity exchanges, i.e., signature of the exchanged particle, and the parity asymmetry is defined as

$$P_{\sigma} \equiv \frac{\sigma^N - \sigma^U}{\sigma^N + \sigma^U} = 2\rho_{1-1}^1 - \rho_{00}^1, \quad (30)$$

where σ^N and σ^U are the contributions of natural and unnatural parity exchanges to the cross section, and we have written P_{σ} in terms of the density matrix elements. So when we have natural parity exchange (like K^* exchange) only, we get $P_{\sigma} = +1$ and we expect $P_{\sigma} = -1$ for unnatural parity exchange (like K exchange) only. Note also that the relation (29) is exact in large energy limit and that there can be some modifications at low energies. Nevertheless, this quantity can give some information on the dominant t -channel exchange process. In helicity conserving processes, the two asymmetries, Σ_V and P_{σ} , have similar values as in our case.

Shown in Fig. 12 are our predictions for the asymmetries P_{σ} and Σ_V . Since they are very sensitive to the spin-parity of the exchanged particle, we can extract informations on the nature of the production mechanisms. For example, if we turn off $K^*N\Theta$ interaction by setting $g_{K^*N\Theta} = 0$, we have only t -channel K exchange. Therefore, we expect $P_{\sigma} = -1$ in this case for both γn and γp reactions. When $g_{K^*N\Theta} \neq 0$, we get t -channel K^* exchange in

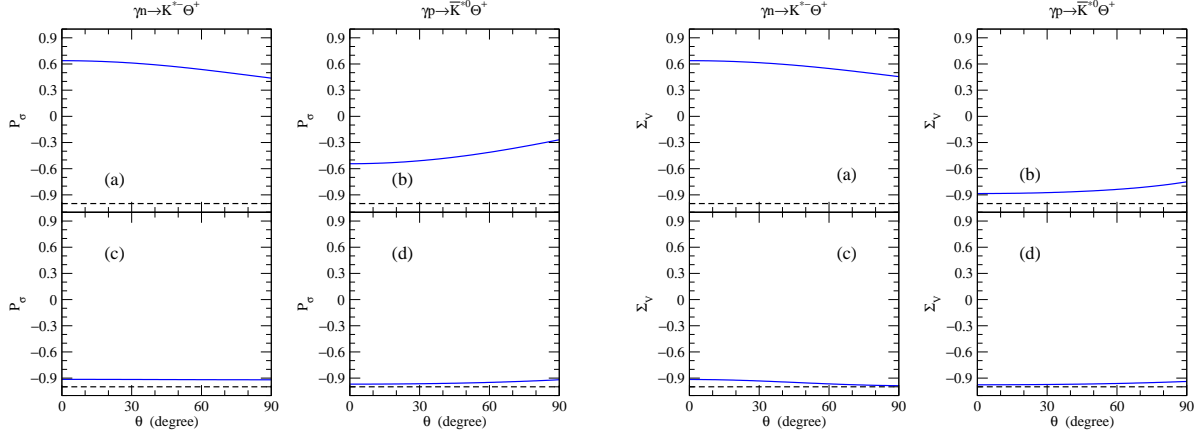


FIG. 12: Parity asymmetry P_σ (left panel) and photon polarization asymmetry Σ_V (right panel) for $\gamma + N \rightarrow \bar{K}^* \Theta^+$ at $E_\gamma = 2.8$ GeV. Notations are the same as in Fig. 5.

the γn reaction, which is, however, not allowed in the γp reaction. In both cases, of course, the s and u channel diagrams can make P_σ deviate from ± 1 , which however does not change the sign of P_σ in the forward scattering angles. Thus we expect that P_σ varies between -1 and $+1$ depending on the relative size of the K and K^* exchanges in the γn reaction, while P_σ is close to -1 in the γp reaction at the forward scattering angles. So measuring P_σ for the γn reaction can give an information on the size of the $K^* N \Theta$ interaction. If it is close to $+1$, the $K^* N \Theta$ coupling would be large and K^* exchange is the dominant process in γn reaction. If it is close to -1 , however, it implies small value of $g_{K^* N \Theta}$. Therefore, measurement of this quantity can test the quark model predictions on $g_{K^* N \Theta} / g_{K N \Theta}$ that has very different values depending on the parity of Θ^+ .

IV. SUMMARY AND DISCUSSION

The recently observed $\Theta^+(1540)$ is believed to be a member of the baryon antidecuplet, but its spin and parity are not confirmed yet. Careful analyses on various Θ^+ production processes are thus expected to give informations on the properties of the $\Theta^+(1540)$ and test various models for hadron structure. As a continuation of our efforts to understand the Θ^+ production processes [47, 48], we have investigated cross sections and spin asymmetries of the $\gamma + N \rightarrow \bar{K}^* + \Theta^+$ reaction in this paper as a complementary process of $\gamma + N \rightarrow \bar{K} + \Theta^+$. In this calculation, the spin of the $\Theta^+(1540)$ is assumed to be $1/2$ and the results are obtained for different assumptions for the parity of the Θ^+ . The obtained cross sections for $\gamma + N \rightarrow \bar{K}^* + \Theta^+$ are found to be comparable to those for $\gamma + N \rightarrow \bar{K} + \Theta^+$. Our results also show that the cross sections for even-parity Θ^+ is much larger than those for odd-parity Θ^+ at least by an order of magnitude.

More solid information for the parity of the observed $\Theta^+(1540)$ could be obtained from the measurements of spin asymmetries. Indeed, within the uncertainties due to the model-dependence of the production mechanisms and the lack of information on several coupling constants, we found that some target-recoil double asymmetries are sensitive to the parity of the Θ^+ at forward scattering angles. But it would be very hard to be measured experimentally because of the difficulties in identifying the nucleon polarization in Θ^+ decay

distribution, which is needed to know the helicity of the Θ^+ . Furthermore, the spin asymmetries depend not only on the parity of Θ^+ but also on the dynamics of the production mechanisms. Thus it would be necessary to measure various spin asymmetries on the proton and neutron targets in order to study the production mechanisms and the parity of Θ^+ . Among various spin asymmetries, the parity asymmetry P_σ in the γn reaction can give a robust information for the dominant t -channel exchange and can be a clean signal for the $K^*N\Theta$ interaction. Once we know the strength of the $K^*N\Theta$ interaction at least qualitatively, we can then learn more about the production processes and the parity of Θ^+ by measuring other spin asymmetries such as single asymmetries and beam-target double asymmetries. When combined with the quark model predictions which lead to $P_\sigma \sim +1$ (-1) for positive (negative) parity Θ^+ in γn reaction, estimation of the $K^*N\Theta$ interaction may also give a clue for the parity of Θ^+ . Such experiments should be possible at current experimental facilities.

Acknowledgments

We are grateful to V. Burkert, H. Gao, A. Hosaka, V. Kubarovsky, T.-S. H. Lee, T. Nakano, B.-Y. Park and E. Smith for fruitful discussions and valuable informations. Y.O. is grateful to the Thomas Jefferson National Accelerator Facility for its warm hospitality. This work was supported by the Brain Korea 21 project of Korean Ministry of Education and by KOSEF under Grant No. 1999-2-111-005-5. The work of Y.O. was supported in part by DOE contract DE-AC05-84ER40150 under which the Southeastern Universities Research Association (SURA) operates the Thomas Jefferson National Accelerator Facility.

-
- [1] LEPS Collaboration, T. Nakano *et al.*, Phys. Rev. Lett. 91 (2003) 012002.
 - [2] DIANA Collaboration, V. V. Barmin *et al.*, Yad. Fiz. 66 (2003) 1763, [Phys. Atom. Nucl. 66 (2003) 1715].
 - [3] CLAS Collaboration, S. Stepanyan *et al.*, Phys. Rev. Lett. 91 (2003) 252001.
 - [4] SAPHIR Collaboration, J. Barth *et al.*, Phys. Lett. B 572 (2003) 127; M. Ostrick for the SAPHIR Collaboration, Talk at Pentaquark 2003 Workshop, Jefferson Lab., 2003.
 - [5] CLAS Collaboration, V. Kubarovsky *et al.*, Talk at CIPANP 2003, New York, 2003, hep-ex/0307088.
 - [6] A. E. Asratyan, A. G. Dolgolenko, M. A. Kubantsev, Yad. Phys. 67 (2004) 704, [Phys. Atom. Nucl. 67 (2004) 682].
 - [7] CLAS Collaboration, V. Kubarovsky *et al.*, Phys. Rev. Lett. 92 (2004) 032001.
 - [8] HERMES Collaboration, A. Airapetian *et al.*, Phys. Lett. B 585 (2004) 213. A. Miller, private communication.
 - [9] NA49 Collaboration, C. Alt *et al.*, Phys. Rev. Lett. 92 (2004) 042003.
 - [10] D. Diakonov, V. Petrov, M. Polyakov, Z. Phys. A 359 (1997) 305.
 - [11] A. V. Manohar, Nucl. Phys. B 248 (1984) 19; M. Chemtob, Nucl. Phys. B 256 (1985) 600; M. Praszalowicz, in *Skyrmions and Anomalies*, edited by M. Jezabek and M. Praszalowicz, (World Scientific, Singapore, 1987), p. 112.
 - [12] H. Weigel, Eur. Phys. J. A 2 (1998) 391.

- [13] F. E. Close, Talk at 10th International Conference on Hadron Spectroscopy, Aschaffenburg, Germany, 2003, hep-ph/0311087.
- [14] R. A. Arndt, I. I. Strakovsky, R. L. Workman, Phys. Rev. C 68 (2003) 042201; nucl-th/0311030.
- [15] H. G. Fischer, S. Wenig, hep-ex/0401014.
- [16] M. Karliner, H. J. Lipkin, hep-ph/0307243; Phys. Lett. B 575 (2003) 249.
- [17] R. Jaffe, F. Wilczek, Phys. Rev. Lett. 91 (2003) 232003.
- [18] Y. Oh, H. Kim, S. H. Lee, Phys. Rev. D 69 (2004) 094009.
- [19] F. E. Close, J. J. Dudek, Phys. Lett. B 586 (2004) 75.
- [20] S. H. Lee, H. Kim, Y. Oh, hep-ph/0402135.
- [21] D. Diakonov, V. Petrov, Phys. Rev. D 69 (2004) 094011.
- [22] E. Shuryak, I. Zahed, Phys. Lett. B 589 (2004) 21.
- [23] R. Bijker, M. M. Giannini, E. Santopinto, hep-ph/0310281, Eur. Phys. J. A (in press).
- [24] Fl. Stancu, D. O. Riska, Phys. Lett. B 575 (2003) 242.
- [25] C. E. Carlson, C. D. Carone, H. J. Kwee, V. Nazaryan, Phys. Lett. B 573 (2003) 101.
- [26] C. E. Carlson, C. D. Carone, H. J. Kwee, V. Nazaryan, Phys. Lett. B 579 (2004) 52.
- [27] L. Ya. Glozman, Phys. Lett. B 575 (2003) 18.
- [28] S. M. Gerasyuta, V. I. Kochkin, hep-ph/0310227.
- [29] H. Walliser, V. B. Kopeliovich, Zh. Eksp. Teor. Fiz. 124 (2003) 483, [J. Exp. Theor. Phys. 97 (2003) 433].
- [30] M. Praszalowicz, Phys. Lett. B 575 (2003) 234.
- [31] N. Itzhaki, I. R. Klebanov, P. Ouyang, L. Rastelli, Nucl. Phys. B 684 (2004) 264.
- [32] B. K. Jennings, K. Maltman, Phys. Rev. D 69 (2004) 094020.
- [33] D. Borisyyuk, M. Faber, A. Kobushkin, hep-ph/0307370.
- [34] S.-L. Zhu, Phys. Rev. Lett. 91 (2003) 232002.
- [35] R. D. Matheus, F. S. Navarra, M. Nielsen, R. da Silva, S. H. Lee, Phys. Lett. B 578 (2004) 323.
- [36] J. Sugiyama, T. Doi, M. Oka, Phys. Lett. B 581 (2004) 167.
- [37] T. D. Cohen, Phys. Lett. B 581 (2004) 175; T. D. Cohen, R. F. Lebed, Phys. Lett. B 578 (2004) 150.
- [38] F. Csikor, Z. Fodor, S. D. Katz, T. G. Kovács, JHEP 0311 (2003) 070. S. Sasaki, hep-lat/0310014; T.-W. Chiu, T.-H. Hsieh, hep-ph/0403020; N. Mathur *et al.*, hep-ph/0406196.
- [39] P. Bicudo, G. M. Marques, Phys. Rev. D 69 (2004) 011503; D. E. Kahana, S. H. Kahana, Phys. Rev. D 69 (2004) 117502; F. J. Llanes-Estrada, E. Oset, V. Mate, Phys. Rev. C 69 (2004) 055203; T. Kishimoto, T. Sato, hep-ex/0312003.
- [40] J. Randrup, Phys. Rev. C 68 (2003) 031903; L. W. Chen, V. Greco, C. M. Ko, S. H. Lee, W. Liu, nucl-th/0308006; J. Letessier, G. Torrieri, S. Steinke, J. Rafelski, Phys. Rev. C 68 (2003) 061901.
- [41] H. J. Lipkin, Phys. Lett. B 195 (1987) 484; C. Gignoux, B. Silvestre-Brac, J. M. Richard, Phys. Lett. B 193 (1987) 323; Fl. Stancu, Phys. Rev. D 58 (1998) 111501; M. Genovese, J.-M. Richard, Fl. Stancu, S. Pepin, Phys. Lett. B 425 (1998) 171.
- [42] C. G. Callan, I. Klebanov, Nucl. Phys. B 262 (1985) 365; Y. Oh, D.-P. Min, M. Rho, N. N. Scoccola, Nucl. Phys. A 534 (1991) 493; D. O. Riska, N. N. Scoccola, Phys. Lett. B 299 (1993) 338; D.-P. Min, Y. Oh, B.-Y. Park, M. Rho, Int. Jour. Mod. Phys. E 4 (1995) 47.
- [43] Y. Oh, B.-Y. Park, D.-P. Min, Phys. Lett. B 331 (1994) 362; Phys. Rev. D 50 (1994) 3350;

- Y. Oh, B.-Y. Park, Phys. Rev. D 51 (1995) 5016.
- [44] W. Liu, C. M. Ko, Phys. Rev. C 68 (2003) 045203.
- [45] W. Liu, C. M. Ko, Nucl. Phys. A 741 (2004) 215.
- [46] S. I. Nam, A. Hosaka, H.-C. Kim, Phys. Lett. B 579 (2004) 43.
- [47] Y. Oh, H. Kim, S. H. Lee, Phys. Rev. D 69 (2004) 014009.
- [48] Y. Oh, H. Kim, S. H. Lee, Phys. Rev. D 69 (2004) 074016.
- [49] W. Liu, C. M. Ko, V. Kubarovsky, Phys. Rev. C 69 (2004) 025202.
- [50] T. Hyodo, A. Hosaka, E. Oset, Phys. Lett. B 579 (2004) 290.
- [51] Q. Zhao, Phys. Rev. D 69 (2004) 053009.
- [52] K. Nakayama, K. Tsushima, Phys. Lett. B 583 (2004) 269.
- [53] A. W. Thomas, K. Hicks, A. Hosaka, Prog. Theor. Phys. 111 (2004) 291.
- [54] S. Capstick, P. R. Page, W. Roberts, Phys. Lett. B 570 (2003) 185.
- [55] KTeV Collaboration, A. Alavi-Harati *et al.*, Phys. Rev. Lett. 89 (2002) 072001.
- [56] M. V. Polyakov, A. Sibirtsev, K. Tsushima, W. Cassing, K. Goeke, Eur. Phys. J. A 9 (2000) 115.
- [57] J. Haidenbauer, G. Krein, Phys. Rev. C 68 (2003) 052201; S. Nussinov, hep-ph/0307357; A. Casher, S. Nussinov, Phys. Lett. B 578 (2004) 124.
- [58] C. E. Carlson, C. D. Carone, H. J. Kwee, V. Nazaryan, hep-ph/0312325.
- [59] H.-C. Kim, M. Praszalowicz, Phys. Lett. B 585 (2004) 99; Y. R. Liu, P. Z. Huang, W. Z. Deng, X. L. Chen, S.-L. Zhu, Phys. Rev. C **69**, 035205 (2004); R. Bijker, M. M. Giannini, E. Santopinto, Phys. Lett. B 595 (2004) 260.
- [60] Y. Oh, A. I. Titov, T.-S. H. Lee, Phys. Rev. C 63 (2001) 025201; Y. Oh, T.-S. H. Lee, Phys. Rev. C 66 (2002) 045201;
- [61] E. Bagán, A. Bramon, F. Cornet, Phys. Rev. D 31 (1985) 2270.
- [62] A. I. Titov, Y. Oh, S. N. Yang, T. Morii, Phys. Rev. C 58 (1998) 2429.
- [63] W. M. Kloet, W.-T. Chiang, F. Tabakin, Phys. Rev. C 58 (1998) 1086.
- [64] K. Schilling, P. Seyboth, G. Wolf, Nucl. Phys. B 15 (1970) 397, (E) 18 (1970) 332.
- [65] G. Cohen-Tannoudji, Ph. Salin, A. Morel, Nuovo Cimento 55 (1968) 412.